Polymer 130 (2017) 10–16

Contents lists available at ScienceDirect

Polymer

journal homepage: www.elsevier.com/locate/polymer

# Barrier, mechanical and conductive properties of polycaprolactam nanocomposites containing carbon-based particles: Effect of the kind of particle

Rodrigo Méndez [a], Benjamin Constant [a], Cristhian Garzon [a], Muhammad Nisar [b], Sônia Marlí Bohrz Nachtigall [b], Raúl Quijada [a, *]

[a] Departamento de Ingeniería Química y Biotecnología, Facultad de Ciencias Físicas y Matemáticas, Universidad de Chile, Beauchef 850, Santiago, Chile
[b] Instituto de Quimica, Universidade Federal do Rio Grande do Sul, Avenida Bento Goncalves 9500, Porto Alegre, Brazil

ARTICLE INFO

*Article history:*
Received 23 May 2017
Received in revised form
22 September 2017
Accepted 28 September 2017
Available online 29 September 2017

*Keywords:*
Polyamide nanocomposites
Graphene oxide
Carbon nanotubes
Barrier properties
Electrical conductivity
Mechanical properties

ABSTRACT

In this study, polycaprolactam (PA6) nanocomposites with thermally reduced graphene oxide (TrGO) and carbon nanotubes (CNTs) were prepared by melt blending with the aim of obtaining films with improvements in permeability (oxygen and water vapor), mechanical properties and electrical conductivity. The permeability to water vapor and oxygen of the nanocomposites containing TrGO significantly decreased with increasing filler load due to a more tortuous path to gas permeation. For CNT nanocomposites, low barrier properties were found. The tensile tests showed similar behavior in both cases, with somewhat higher elastic modulus for TrGO compounds. CNT gave higher electrical conductivity to polyamide with lower percolation threshold; however this conductivity reached a constant value around 10 wt% of filler. The conductivity of TrGO nanocomposites was lower, probably due to the presence of impurities in its structure; however, the property increased up to 15 wt% of filler load without evidence of stabilization at this concentration.



## 1. Introduction

The packaging industry has the purpose of generating tools that allow the consumer to obtain the products in optimal conditions. Dealing with food, this means preserving its physical, chemical, biological, and nutritional characteristics. That is why the materials used for packaging foods must have some specific physicochemical properties such as, for example, low permeability to gases (mainly oxygen and/or moisture) and adequate mechanical properties (resistance to breakage, for instance). It is well known that the presence of gases affect the taste, smell, color, appearance, among others, caused by the chemical and metabolic degradation of the food [1].

Due to their functionality, light weight, easy processing, and low cost, polymers have replaced conventional materials used for packaging for more than 20 years. The most widely used polymers in food packaging are polyethylene (PE), polypropylene (PP), polystyrene (PS), poly(ethyleneterephthalate) (PET), and polyamide (PA). However, despite their high versatility, there is a limit in the properties that polymeric materials used in food packaging can have in terms of permeability to gases like oxygen and water vapor. The mechanical and barrier properties can be changed significantly when nanoscaled materials such as clay and graphene are incorporated. Depending on the aspect ratio and dispersion of the fillers, the permeability of some gases could be hindered and the mechanical properties can be improved [2–4].

Among the large variety of nanofillers used for technological applications, carbon-based materials stand out, particularly one-dimensional (1D) carbon nanotubes (CNTs), due to their exceptional properties such as thermal stability (>700 °C in air), mechanical resistance (50 GPa), and electrical conductivity (~$10^6$ S/m). The presence of CNTs are thought to increase the tortuosity in polymer nanocomposite films leading to slower diffusion processes and hence, to a lower permeability. However, due to their high cost, alternative less expensive nanostructures have been sought recently, such as, for example, graphite and its derivatives. Graphite has the most stable carbon structure under standard conditions, and it is a low-cost natural material. Nanostructures obtained from graphite, like graphene and its derivatives, are the fillers with the

* Corresponding author.
*E-mail address:* raquijad@ing.uchile.cl (R. Quijada).

https://doi.org/10.1016/j.polymer.2017.09.063
0032-3861/

highest potential for replacing costly CNTs [5]. Graphene has extraordinary properties, with a Young's modulus of 1 TPa and a tensile strength of 130 GPa, which turn it into the strongest material created so far. These properties, together with its large specific surface area (~2630 $m^2/g$) and impermeability to gases, show the great potential of graphene for using as filler to improve the properties of polymers [6]. Recently our research group has been working on the use of strong oxidizing agents to produce exfoliated graphite oxide particles bearing hydroxyl and epoxide functional groups. Such functional groups largely reduce the thermal stability and the electrical conductivity of the material. However, they can be restored by a thermal shock at high temperatures in inert atmosphere, which gives the thermally reduced graphene oxide (TrGO). This TrGO is a nanosized form of graphite that seems to be an excellent substitute of CNTs in polymer nanocomposites considering that the amount of polar groups in its structure can be modulated to allow an adequate adhesion with different polymers [7].

Many polymer matrices have been used to develop nanocomposites with nanoparticles based on clays (montmorillonites) and carbon (specifically graphene and its derivatives). Among them, nylon 11 [8], polypropylene (PP) [9], polycarbonate (PC) [10], polystyrene (PS) [11] should be mentioned.

In food packaging industry, polyamides like polycaprolactam are the most widely used because they are characterized by having excellent mechanical properties, great hardness, chemical resistance (except to strong acids and bases), thermal stability (up to 180 °C), and good barrier properties for different gases, such as oxygen, but not for water vapor, and as a consequence, multilayer package is usually used, which utilizes different polymers to prevent the passage of these gases [12]. In addition, in the literature it was found that using a nanoparticulate material as filler allows getting the same or better properties as different polymer layers [3]. R. Scaffaro et al. [13–15] has reported several works where the elastic modulus in PA6/CNTs nanocomposites has been improved, reaching improvements up to approximately three times higher than that of neat PA6 with functionalized CNTs. These enhancements were due to a good dispersion and adhesion between the CNTs and the PA6. In permeability, Tseng et al. [16] found that in polyamide/GO nanocomposites, the water vapor permeability was reduced dramatically by 83% at only 0.001 wt% as a result of an increase in the tortuosity in the nanocomposite due to a good distribution of GO in the polymer matrix.

In the present work has the goal of obtaining polycaprolactam (PA6) nanocomposites containing nanostructures based on carbon, specifically CNTs and TrGO, by melt mixing in order to compare these carbon nanoparticles and contribute to the understanding of how the presence of these particles affects the barrier and mechanical properties as well as the electrical conductivity of these polymer nanocomposites.

## 2. Materials and methods

### 2.1. Materials

A commercial grade polycaprolactam (PA6) Ultramid B33 L, made by BASF (Chile), which has a density of 1150 $kg/m^3$, a melt flow index (MFI) of 5.9 g/10 min, a melting point of 220 °C, and a Young's modulus of 2800 MPa was used as the matrix. Thermally reduced graphene oxide (TrGO) at 600 °C with a surface area of ~261 $m^2/g$ synthesized according to reference [5], and commercial carbon nanotubes (CNTs) of the multiwall type (Baytubes C150P) supplied by Bayer Material Science were used as fillers. Both matrix and CNTs were used as received.

### 2.2. Preparation of nanocomposites

The nanocomposites were prepared by the melt blending technique in a Brabender PlastiCorder double screw mixer, at 260 °C and 100 rpm, in a nitrogen atmosphere. Approximately 30 g per batch of a mixture containing PA6, CNTs and/or TrGO filler was processed for ten minutes. The filler's concentration varied over a range of 1%–15% by weight. The PA6, CNTs and TrGO were dried in a vacuum oven at 80 °C for 16 h prior to be mixed.

### 2.3. Morphology

The morphology and microstructure of the nanocomposites and nanoparticles were studied by transmission electron microscopy (TEM) using a JEOL JEM-1200 Exll system operating at 80 kV. Samples were prepared using an ultramicrotome RMC CXL.

### 2.4. Permeability to oxygen and water vapor

The permeability to oxygen was analysed by the Time Lag method in a permeability cell built in our laboratories, according to a design described elsewhere [4,17,18]. The system was hermetically sealed and exposed to vacuum ($10^{-3}$ bar) for 3 h before running the tests. The permeability to water vapor was measured by the dry cup method [19]. The mass of the cups was measured every 24 h for 15 days.

### 2.5. Mechanical properties

The mechanical properties of the polymeric nanocomposites were studied by tensile tests according to the ASTM D638-10 standard [20] using an HP D500 dynamometer. For this test, bone-shaped samples of total length 120 mm, 80 mm distance between jaws, 10 mm long and 1 mm thick narrow section were tested at a speed of 50 mm/min, at ambient temperature. The results are the average values of five measurements (typical deviation ca. 5%).

### 2.6. Electrical conductivity

The electrical conductivity measurements were made by the standard two-point method, measuring the resistivity of the samples with a Megger BM11 megohmmeter at a maximum voltage of 1200 V.

## 3. Results and discussion

### 3.1. Morphology

Fig. 1 shows TEM images of the polyamide nanocomposites containing 1%, 5% and 10 %wt of CNTs (Fig. 1a, b and c) and 1%, 5% and 10 %wt of TrGO (Fig. 1d, e and f). In the case of the compounds with CNTs, agglomerations are not seen along the polymer matrix; however, for higher filler loadings it is possible to observe some clusters of CNTs. In general, in all the samples the filler is well dispersed in the polymer matrix. This is likely due to the adequate matrix viscosity and processing conditions. The individual multiwalled nanotubes are easily recognizable as long hollow fibers with a diameter of 5–10 nm. Similar structures of CNTs in a polyamide matrix have been observed by Meincke et al. [21]. On the other hand, for the same magnification, some agglomerations are observed in the nanocomposites containing TrGO, despite the presence of residual functional groups on their surface that could promote a better affinity between the matrix and the nanoparticles. The observed result could be due to an incomplete exfoliation of graphite during the previous oxidant/reductive processes. It is

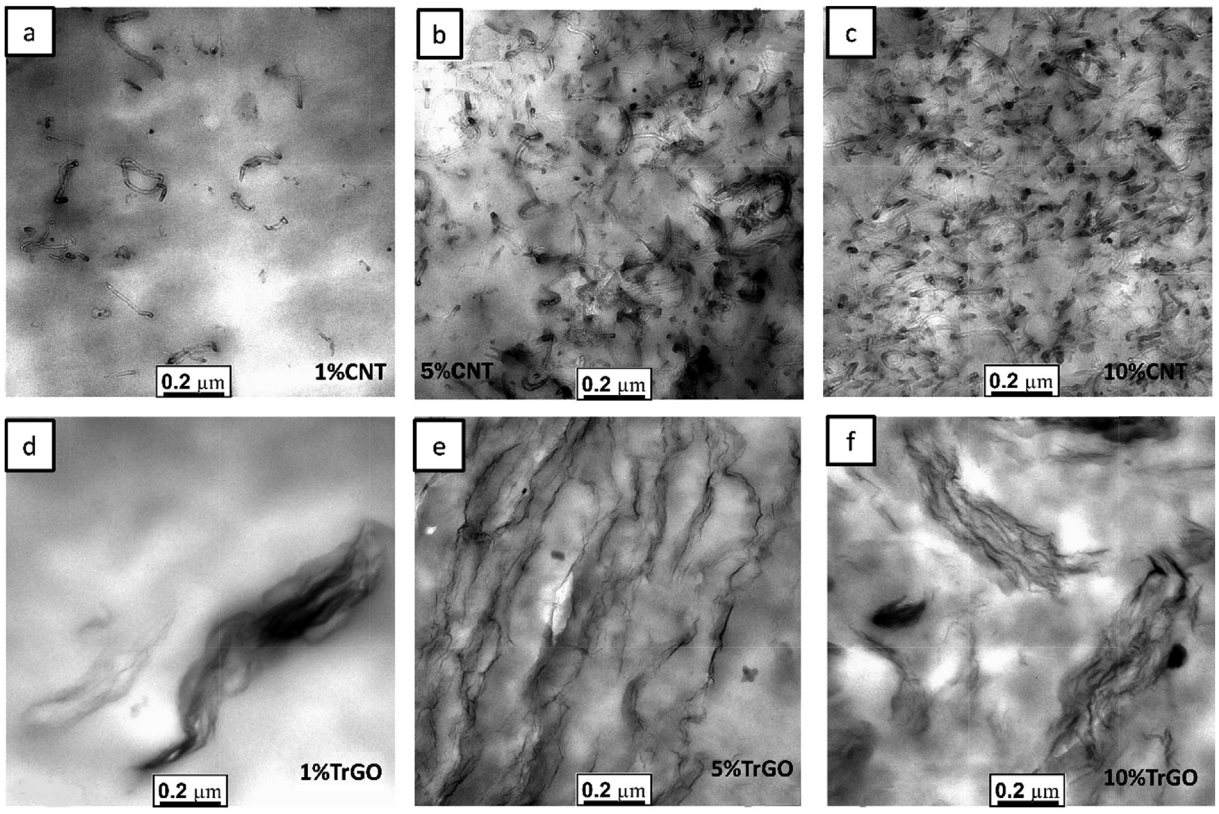


**Fig. 1.** TEM images of a)PA-1wt%CNT, b) PA-5wt%CNT, c) PA-10 wt%CNT, d) PA-1wt%TrGO, e) PA-5wt%TrGO, and f) PA-10 wt%TrGO.

noteworthy that the polyamide 6 generally present poor affinity towards graphene-based fillers since the PA6 is a polar polymer and the graphene-based nanoparticles are highly hydrophobics [22]. Furthermore, it has been reported that the incorporation of GO in polyamide by the melt process can produce buckling, restacking, pleating or folding of the GO nanosheets during the process as a result of intermolecular reactions between oxygen moieties of the GO, mechanical distortion of the lamella structure under shear stress, evaporation of the water within the GO structure, among others [22,23]. Nevertheless, thin platelets and individual layers of filler are also found in the samples, which can be useful to improve the mechanical properties of the polymer matrix.

### 3.2. Permeability to oxygen and water vapor

The results of the permeability to oxygen and water vapor are presented in Fig. 2. To a better understanding of the barrier properties of these nanocomposites, theoretical models were used. Calculated theoretical curves are also shown in the Fig. 2. The modified Felske Model (F-M) was considered in order to study the permeability results of nanocomposites with CNTs, since this model predicts an increase of permeability with filler loadings. This model predicts an increase of the permeability due to the void's formation in the polymer–particle interface by a weak interaction between them as is the case of these systems based on a polar matrix (polyamide) and an apolar filler (CNTs) [24,25]. On the other hand, the Nielsen Model (N-M) was used for the systems with TrGO. This model relates the permeability to the formation of a percolating network of platelets which can provide a more tortuous path that inhibits molecular diffusion through the matrix, and therefore, it predicts a decrease in the permeability [26,27].

It was verified that the CNTs showed an unexpected behavior for low and high nanofiller loading with respect to the permeation of oxygen (Fig. 2a). At 1 wt% of CNTs the permeability decreased almost 80%; however with an increase of the CNTs, the permeability showed an abrupt rise, going up to more than 600% at 15 wt% of them. A similar behavior was found for the water vapor permeability, as shown in Fig. 2b. Other systems described in the literature behaved in a similar way. Alexandre and collaborators [28] found that polyamide/clay nanocomposites showed good barrier properties at low filler contents but loose this property with increasing the filler load. The authors concluded that the decrease in the permeability at low filler load was in accordance with a more tortuous path for gas permeation. However, for high filler load, the barrier effect could be lost because of several concomitant effects such as changes in the physical state of the matrix (size and orientation of crystallites and crystallinity ratio principally) due to the presence of the filler, contribution of the filler/matrix interface to permeability and/or reduction of the molecular mobility as a result of chain confinement effects. These effects could be the responsible of the permeability's results. In addition, the low affinity between the matrix and the CNTs could potentiate the above mentioned effects.

Considering the dispersion of CNTs in polymer matrices, Khan et al. [29] also verified that nanocomposites of polycaprolactam showed better barrier properties to water vapor for low CNTs contents, from 0.05 to 0.5%, which was explained by the increase in tortuosity which led to a slower diffusion. On the contrary, Kim et al. [30] observed larger water flux in PA membranes containing ~0.1 wt% of CNTs in comparison with the PA membrane without CNTs. The authors believed that a good dispersion of the CNTs in the polyamide offered a fast transport way to pass the water molecules, which could go into the inside of the CNTs by capillary forces, passing through the hydrophobic inner side of the filler. On the

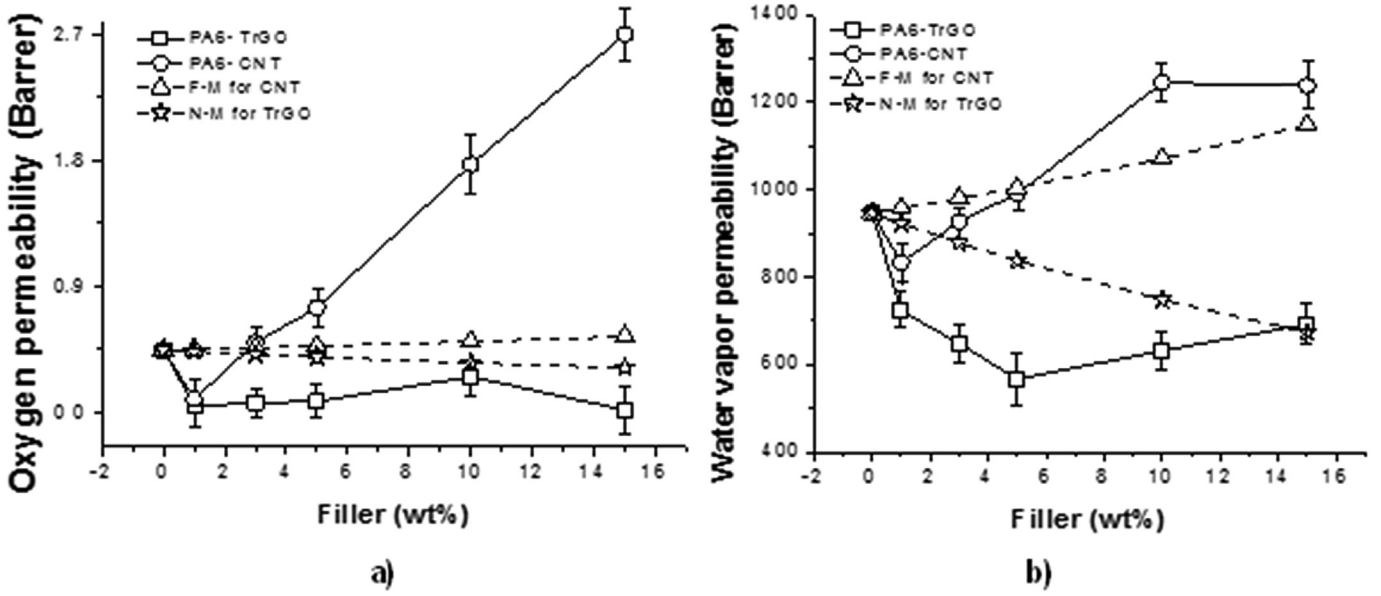


**Fig. 2.** Permeability to oxygen (a) and water vapor (b) - Experimental and theoretical results using the modified Felske Model (F–M) for CNT and the Nielsen Model (N–M) for TrGO filled polycaprolactam.

other hand, high filler loads can result in agglomeration as it was observed in the Fig. 1 and this may also have a deleterious outcome on the barrier properties giving a rise to new pathways for gas diffusion [31].

The permeability usually proceeds by a solution-diffusion mechanism in which it can be calculated using $P = S \cdot D$ [31,32], where S and D denote the solubility and diffusivity of the permeating species, respectively. This relation provides a good basis for a conceptual understanding of the basic principles of permeability through polymer films. Once the penetrant molecule has adsorbed onto the surface of the polymer, it must dissolve in the polymer matrix and then diffuse down a concentration gradient through the film, before desorbing from the opposite surface. As a consequence, the differences between the nature of the gases (oxygen and water vapor) could be also contributed to the permeabilities obtained since they have different solubilities. This can also explain in our results that the oxygen permeability was increased more than the water vapor permeability likely due to the polarity of the permeant species. Thus, the solubility of oxygen (apolar gas) in PA6 matrix can be increased as a result of the apolar nanoparticles (CNTs) incorporated since they could decreased the hydrophobicity of the PA6 matrix.

Certainly, the dual behavior of the PA6-CNT nanocomposites with respect to oxygen and water vapor permeation can reflect competitive ways of gas diffusion in the systems where only very low amounts of filler are able to improve the barrier properties.

It was observed that the theoretical results calculated for the oxygen permeability of CNT nanocomposites using the F-M were significantly lower than the experimental results. This was likely due to the geometry of the CNTs, which have a high aspect ratio favoring the formation of preferential channels where the permeating species could go through the matrix easier, increasing the permeation. In addition, the TEM images showed a good dispersion of the CNTs, where it can even facility more the path through the matrix. In general, nanoparticles with cylindrical geometry favor the formation of these channels, and this is increased with the filler load [18,30].

Considering the nanocomposites containing TrGO, it was verified that this filler continuously decreased the permeation to oxygen (Fig. 2a). At 1 wt% of TrGO the permeability to oxygen decreased around 90%, while at 15 wt% of TrGO it was reduced ~97%, reaching almost zero in permeability. Graphene has been considered the most impermeable material known [33]. According the literature, defect-free graphene is impermeable even to very small structures such as helium atoms because of its high aspect ratio and the high electronic density of the carbon rings [3]. As the increase of graphene load in the PA6 matrix produced an increase in the oxygen barrier properties, it is possible to suppose that the filler is sufficiently well dispersed giving a more tortuous path for the gas permeation. It is already established that barrier properties are enhanced with the filler load when it is well dispersed in the polymeric matrix [21]. Probably, the dispersion of the TrGO in the polyamide was helped by the improved adhesion among the components after the pretreatment used to expand the graphite. This pretreatment introduced functional polar groups in the filler structure which could increase adhesion with the polar polymer matrix. In this case, the solubility to apolar gases such as oxygen in the polar PA6 matrix should increase the permeability since the presence of some residual oxygen groups in the surface of the TrGO nanoparticles; however the permeability showed a significant decrease, which lead to assume that in this case the solubility has not an effect.

For water vapor permeability, a significant reduction was found up to 5% of filler because of the higher tortuous path for the permeant specie. From this concentration on a small loose in permeability was found. According to the literature (Alexeandre [28]), interactions among the nanocomposite and water can increase the free volume in the polymer phase through polymer plasticization, favoring the chain segment mobility. This effect depends on the local water concentration and increases diffusion. We do believe that high water concentration can plasticize the material, increasing the water vapor permeation. However, it was verified that up to 15 %wt of TrGO, the water vapor permeability was always lower in the nanocomposites than for the pure polymer matrix. In addition, the decrease in the water vapor permeability of the nanocomposites with TrGO could be also attributable to a change of solubility due to the hydrophobic TrGO, suggesting that the water vapor (polar molecule) solubility in the nanocomposites can be

decreased compared to the hydrophilic pure PA6.

The application of the N-M for the TrGO nanocomposites resulted in values of permeability higher than the experimental ones for both oxygen and water vapor permeation. This is because the N-M does not consider the functional groups present in the matrix and in the TrGO, which causes good affinity between them and makes the diffusion of the permeating agent to take longer to go through the matrix. Moreover, this model does not take in account changes in the physical state of the matrix after filler addition (size and orientation of crystallites, crystallinity ratio, etc.), the contribution of the filler/matrix interface to permeability, neither the reduction of the molecular mobility due to chain confinement [28]. Such changes may affect the barrier properties, deviating the experimental results from the theoretical values.

The findings in permeability suggest that the gas barrier performance of polymer nanocomposites is determined by mainly three factors: filler properties (nature of the nanoparticles, resistance to gas diffusion, aspect ratio, and volume fraction), the intrinsic barrier property of the polymer matrix, and the quality of dispersion (agglomeration, free volume, orientation of filler platelets, etc.). In particular, considering the oxygen and water vapor barrier properties, the addition of TrGO to the polyamide matrix showed to have a better effect than the addition of CNTs. As TrGO is a nanofiller more easily obtained, coming from natural resources that are abundant in the earth, this strategy is very promising to improve the properties of films that will be used in applications requiring low gas permeability such as in food packing.

### 3.3. Mechanical behavior of the nanocomposites

The effects of CNTs and TrGO on the Elastic modulus and on the deformation at break of the nanocomposites are shown in Fig. 3.

It was seen that the elastic modulus increased with the filler content, and this rise was greater for the TrGO nanocomposites. Fig. 3a shows that the elastic modulus for TrGO compounds was increased up to 58.8% at 10 wt%, while for CNTs it was risen up to 24.8% at 10 wt% as well. These increases can be due to the addition of rigid nanoparticles, such as CNTs and TrGO, to polymer matrices which can easily improve the modulus since the rigidity of inorganic fillers is generally much higher than that of the organic polymers, a phenomenon known as load transfer mechanism. R. Scaffaro et al. [13] reported an increase in the elastic modulus of approximately 33% with 2 wt% of CNTs in PA6. Furthermore, when the CNTs were functionalized with oxygenated moieties (fCNTs), the elastic modulus was risen up to 107% at 2 wt% due to that the fCNTs have polar groups on their surface and they are likely more adherent and well dispersed in the PA6 matrix. The largest increase shown by the nanocomposite materials with TrGO can be explained by the stronger adhesion between the polyamide matrix and these fillers due to the presence of oxygenated residual groups obtained after the oxidative/thermal treatment of graphite, similar trend to the improvements reported with the fCNTs. Moreover, the rough and wrinkled texture and the presence of defects in the filler particles also increase the mechanical link with the matrix. This trend was similar to those reported by other authors using carbon-based fillers in polypropylene and polyamide matrices [9,34,35]. The enhancements in the elastic modulus could be also due to changes in crystallinity of the nanocomposites. It is well-known that the incorporation of nanoparticles in PA6 can had a profound effect on the crystallization due to the fact that they act as heterogeneous nucleating agents and accelerate the formation of α-phase crystals with the absence of γ-phase crystals [32,36,37]. This occurs because the nanoparticles accelerate the crystallization of the matrix and the α-phase crystals constituted the most thermodynamically stable phase in PA6 with a faster growth rate [32,38,39]. Logakis et al. reported an enhancement in the mechanical properties in PA6/CNTs nanocomposites due to two factors; the conversion of the γ phase crystals to α-phase crystals, and from the transfer of stress from the PA6 to the CNTs. This behavior has been also found in PA6/clays nanocomposites [32]. However, in this work the crystallinity of these nanocomposites was not studied and deserves a further analysis. It is interesting to observe that the elastic modulus showed a tendency to increase at low loads and then it reached a plateau in both cases. The stabilization of Young's modulus was around 5 wt% for CNTs and around 10 wt% for TrGO nanocomposites.

With respect to elongation at break, it was verified that the behavior of TrGO and CNT nanocomposites was very similar. From Fig. 3b it is possible to see that the property showed a fast decrease for low concentration of both fillers, falling to around 91.3% for 3 wt % of CNTs and 5 wt% of TrGO. The marked decrease in the elongation at break in these nanocomposites is likely due to the fact that the nanoparticles are much stiffer than the PA6 matrix; in fact the filling materials have virtually no deformation due to its high stiffness [18]. In addition, these nanoparticles strongly restrict the polymer chain movement of the polymer chains when it is

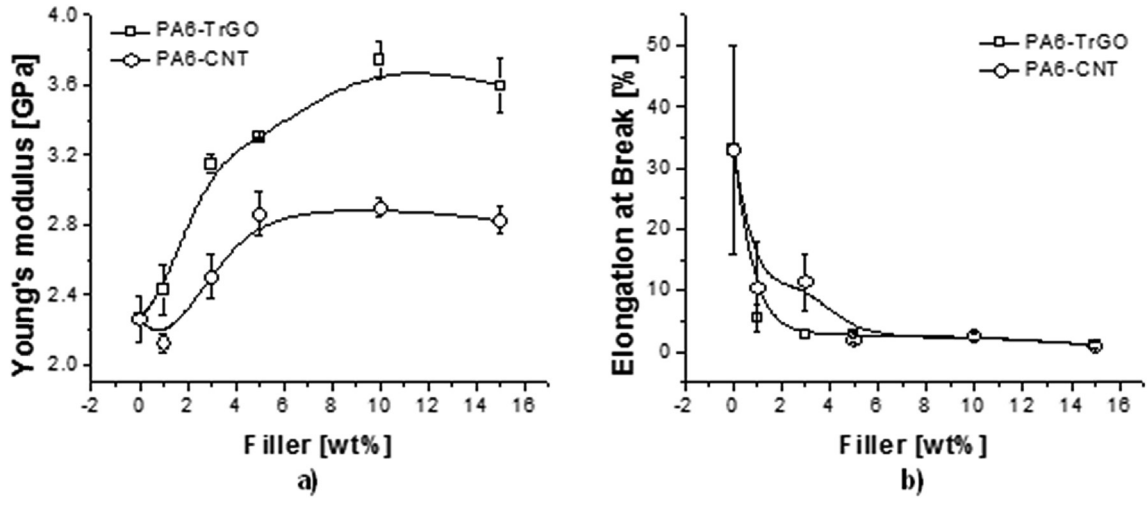


**Fig. 3.** Mechanical properties of PA-CNT and PA-TrGO: a) Young's modulus, and b) deformation at break.

subjected to stress. This restriction prevented them from stretching, thereby reducing the elongation [18,40,41].

### 3.4. Conductivity behavior

Fig. 4 shows the electrical conductivity variations of the nanocomposites at different CNTs and TrGO loads in PA6.

Significant differences are clearly seen in terms of the minimum concentration required for each conductive filler (CNT or TrGO) to achieve conductivity changes, a concentration known as the electrical percolation threshold. CNT compounds presented a lower electrical percolation threshold (~2 wt%), characterized by a drastic increase of the material's conductivity, reaching values in the order of ~$10^{-5}$ S/m with only ~3 wt% of CNT, thereby giving rise to a semiconductor material. For TrGO compounds, the electrical percolation threshold appeared around 5 wt%, achieving the conductivity of a semiconductor material when the filler percentage was greater than 10 wt%. Furthermore, the maximum electrical conductivity achieved in each case can have differences of up to three orders of magnitude. The great difference in terms of conductive properties presented by these nanocomposites containing different carbon-based fillers is due to the fact that the TrGO may contain impurities in its structure, such as reminiscent oxygen-bearing functional groups (produced by the previous oxidative process), which do not allow a good electrical conductivity within the matrix. In addition, it has been reported that incomplete oxidation and exfoliation of GO and agglomerations of graphene nanosheets can result in low electrical conductivities [42], and both incomplete exfolation and agglomerations were observed in the Fig. 1 (d, e and f). On the other hand, the CNTs have high purity and a cylindrical structure which facilitate the formation of a continuous percolated network throughout the matrix, with preferential channels through which the electrons can freely travel [43]. In addition, the Fig. 1 (a, b and c) showed a better dispersion of the CNTs in the polymer matrix, which can contribute in the formation of preferential channels in the polymeric matrix.

The results of conductivity obtained for the CNT and TrGO nanocomposites are similar to those reported by other studies [5,44–46]. In our study, we observed that the CNT compounds showed the lowest percolation threshold and the highest electrical conductivity. However, this conductivity reached its maximum at 10 wt% of CNTs and did not increase at all above this load. On the other hand, TrGO nanocomposites showed the highest conductivity at the highest load tested (15 wt%); however it did not appear to be stabilized at this concentration. This behavior suggests that, if necessary, higher loads of this inexpensive filler could improve even more the electrical conductivity in PA6/carbon-based nanocomposites. These carbon based nanocomposites could have significant applications in hot areas at present, especially in electrode materials, solar cells, and supercapacitors [47]. Moreover, these carbon based nanoparticles can be been prepared by combining CTNs or TrGO with other materials, such as metals and semiconductors in order to have a wider range of applications. Another application can be sensors since graphene has a huge theoretical surface area, in which all atoms of a single-layer graphene sheet could be exposed to the air. Accordingly, they can adsorb gas molecules and provide the extraordinary sensing sites per unit volume [6,48]. In the case of CNTs, in the last decade, they have been usually combined with metal oxides such as aluminum dioxide, titanium dioxide, zinc oxide, iron oxide, among others and applied toward novel devices with remarkable properties for an extensive range of applications [49]. Therefore, the findings in this work could be a step in the understanding and development of future applications.

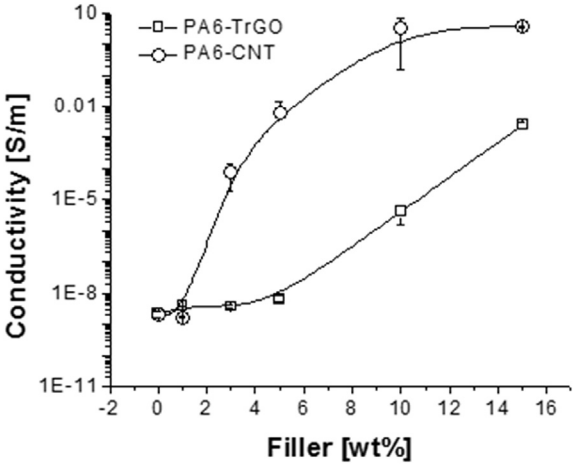


**Fig. 4.** Electrical conductivity of the PA-CNT and PA-TrGO nanocomposites at different loads.

## 4. Conclusions

Polyamide nanocomposites containing carbon nanotubes (CNTs) and thermally reduced graphene oxide (TrGO) were prepared by melt mixing. TEM images indicated that the CNTs were well dispersed in the polymer matrix. On the other hand, TrGO were also well distributed in the matrix, although it showed some non-exfoliated structures, which it is probably as a result of the previous treatment used for graphite exfoliation and due to a restacking of the TrGO nanosheets during the melt process.

In barrier properties, the addition of TrGO to the polyamide showed a remarkable decrease to oxygen and water vapor permeabilities, reaching a 90% of reduction with just 1 wt% and almost zero at 15 wt% of TrGO in oxygen permeability with similar a trend in the water vapor permeability. This behavior can be related to the existence of a more tortuous path for the gas through the matrix and to the nature of the TrGO. On the other hand, the addition of CNTs to the polyamide slightly decreased oxygen and water vapor permeabilities up to ~3 wt%, increasing rapidly the permeation of these gases above this concentration. This behavior was likely as a result of the formation of preferential channels at the nanotubes surfaces, which facilitated the gas permeation.

Regarding the mechanical properties, CNTs and TrGO fillers increased the stiffness in the polyamide due to the load transferred, and the deformation at break was considerable reduced since the nanoparticles strongly restrict the polymer chain movements when under stress.The conductivity tests indicated that CNTs gave rise to semiconductive materials at low concentration (around ~3%); however the conductivity reached its maximum at ~10 wt% of CNTs. TrGO nanocomposites only achieved semiconductive properties at 10 wt%. The conductivity of TrGO compounds was always lower than that of the CNT compounds for the same filler loadings, however it did not seemed to be stabilized at the highest load tested (15 wt%). Such behavior suggests that, if necessary, higher concentrations of TrGO may be used to increase the conductivity.

The results point to a good perspective regarding the use of TrGO in polyamide, aiming to obtain films with barrier properties superior to those obtained in similar nanocomposites containing CNTs. The materials can also show good electrical conductivity and excellent mechanical properties. Furthermore, for future works, it is recommended to study and analyze the crystallinity since it plays a crucial role in PA6 nanocomposites.

## Acknowledgment

To CONICYT for supporting Project FONDECYT 1160521, Mr. Moisés Gómez for helping in the manuscript and also in the discussion of the results and Professor Carlos Bergmann from the Departamento de Engenharia dos Materiais of the Universidade Federal do Rio Grande do Sul, Porto Alegre, Brazil for TEM analysis.

## References

[1] C. Silvestre, D. Duraccio, S. Cimmino, Food packaging based on polymer nanomaterials, Prog. Polym. Sci. 36 (12) (2011) 1766–1782.
[2] I. Zaman, et al., From clay to graphene for polymer nanocomposites—a survey 21 (2014) 429.
[3] Y. Cui, S.I. Kundalwal, S. Kumar, Gas barrier performance of graphene/polymer nanocomposites, Carbon 98 (2016) 313–333.
[4] V.N. Dougnac, R. Alamillo, B.C. Peoples, R. Quijada, Effect of particle diameter on the permeability of polypropylene/SiO2 nanocomposites, Polymer 51 (2010) 2918–2926.
[5] C. Garzón, H. Palza, Electrical behavior of polypropylene composites melt mixed with carbon-based particles: effect of the kind of particle and annealing process, Compos. Sci. Technol. 99 (0) (2014) 117–123.
[6] H. Kim, A.A. Abdala, C.W. Macosko, Graphene/polymer nanocomposites, Macromolecules 43 (16) (2010) 6515–6530.
[7] J. Riquelme, et al., Development of multifunctional polymer nanocomposites with carbon-based hybrid nanostructures synthesized from ferrocene, Eur. Polym. J. 75 (2016) 200–209.
[8] D. Yuan, et al., Unusual toughening effect of graphene oxide on the graphene oxide/nylon 11 composites prepared by in situ melt polycondensation, Compos. Part B Eng. 55 (2013) 215–220.
[9] C. Garzon, et al., Effect of carbon-based particles on the mechanical behavior of isotactic poly(propylene)s, Macromol. Mater. Eng. 301 (4) (2016) 429–440.
[10] H. Kim, C.W. Macosko, Processing-property relationships of polycarbonate/graphene composites, Polymer 50 (15) (2009) 3797–3809.
[11] R. Haggenmuller, et al., Production and characterization of polymer nanocomposites with highly aligned single-walled carbon nanotubes, J. Nanosci. Nanotechnol. 3 (1–2) (2003) 105–110.
[12] T.V. Duncan, Applications of nanotechnology in food packaging and food safety: barrier materials, antimicrobials and sensors, J. colloid interface Sci. 363 (2011) 1–24.
[13] R. Scaffaro, A. Maio, Enhancing the mechanical performance of polymer based nanocomposites by plasma-modification of nanoparticles, Polym. Test. 31 (7) (2012) 889–894.
[14] R. Scaffaro, A. Maio, A.C. Tito, High performance PA6/CNTs nanohybrid fibers prepared in the melt, Compos. Sci. Technol. 72 (15) (2012) 1918–1923.
[15] R. Scaffaro, et al., Plasma Functionalization of Multiwalled Carbon Nanotubes and Their Use in the Preparation of Nylon 6-Based Nanohybrids, Plasma Process. Polym. 9 (5) (2012) 503–512.
[16] I.H. Tseng, et al., Transparent polyimide/graphene oxide nanocomposite with improved moisture barrier property, Mater. Chem. Phys. 136 (1) (2012) 247–253.
[17] D. Bracho, et al., Functionalization of Silica Nanoparticles for Polypropylene Nanocomposite Applications, J. Nanomater. 2012 (Article ID 263915) (2012) 8.
[18] M. Gómez, et al., Effect of morphology on the permeability, mechanical and thermal properties of polypropylene/SiO2 nanocomposites, Polym. Int. 64 (9) (2015) 1245–1251.
[19] ASTM, E96/E96M-10: Standard Test Methods for Water Vapor Transmission of Materials.
[20] ASTM, ASTM D 638-00: Standard Test Method for Tensile Properties of Plastics.
[21] O. Meincke, et al., Mechanical properties and electrical conductivity of carbon-nanotube filled polyamide-6 and its blends with acrylonitrile/butadiene/styrene, Polymer 45 (3) (2004) 739–748.
[22] A. Maio, et al., A novel approach to prevent graphene oxide re-aggregation during the melt compounding with polymers, Compos. Sci. Technol. 119 (2015) 131–137.
[23] R. Scaffaro, A. Maio, A green method to prepare nanosilica modified graphene oxide to inhibit nanoparticles re-aggregation during melt processing, Chem. Eng. J. 308 (2017) 1034–1047.
[24] S.a. Hashemifard, F.a. Ismail, T. Matsuura, Prediction of gas permeability in mixed matrix membranes using theoretical models, J. Membr. Sci. 347 (2010) 53–61.
[25] V.N. Dougnac, B.C. Peoples, R. Quijada, The effect of nanospheres on the permeability of PA6/SiO2 nanocomposites, Polym. Int. 60 (11) (2011) 1600–1606.
[26] A. Saritha, et al., State of the Art – Nanomechanics, in Polymer Composites, Wiley-VCH Verlag GmbH & Co. KGaA, 2013, pp. 1–12.
[27] L.E. Nielsen, Models for the Permeability of Filled Polymer Systems, J. Macromol. Sci. Part A - Chem. 1 (1967) 929–942.
[28] B. Alexandre, et al., Water barrier properties of polyamide 12/montmorillonite nanocomposite membranes: Structure and volume fraction effects, J. Membr. Sci. 328 (1) (2009) 186–204.
[29] R.A. Khan, et al., Mechanical and barrier properties of carbon nanotube reinforced PCL-based composite films: Effect of gamma radiation, J. Appl. Polym. Sci. 127 (5) (2013) 3962–3969.
[30] H.J. Kim, et al., High-Performance Reverse Osmosis CNT/Polyamide Nanocomposite Membrane by Controlled Interfacial Interactions, ACS Appl. Mater. Interfaces 6 (4) (2014) 2819–2829.
[31] B. Tan, N.L. Thomas, A review of the water barrier properties of polymer/clay and polymer/graphene nanocomposites, J. Membr. Sci. 514 (2016) 595–612.
[32] M. Gómez, H. Palza, R. Quijada, Influence of Organically-Modified Montmorillonite and Synthesized Layered Silica Nanoparticles on the Properties of Polypropylene and Polyamide-6 Nanocomposites, Polymers 8 (11) (2016) 386.
[33] V. Berry, Impermeability of graphene and its applications, Carbon 62 (2013) 1–10.
[34] R. Sengupta, et al., A review on the mechanical and electrical properties of graphite and modified graphite reinforced polymer composites, Prog. Polym. Sci. 36 (5) (2011) 638–670.
[35] P. Steurer, et al., Functionalized Graphenes and Thermoplastic Nanocomposites Based upon Expanded Graphite Oxide, Macromol. Rapid Commun. 30 (4–5) (2009) 316–327.
[36] E. Logakis, et al., Structure–property relationships in polyamide 6/multi-walled carbon nanotubes nanocomposites, J. Polym. Sci. Part B Polym. Phys. 47 (8) (2009) 764–774.
[37] X. Zhang, et al., Facile preparation route for graphene oxide reinforced polyamide 6 composites via in situ anionic ring-opening polymerization, J. Mater. Chem. 22 (45) (2012) 24081–24091.
[38] B. Guo, et al., Crystallization behavior of polyamide 6/halloysite nanotubes nanocomposites, Thermochim. Acta 484 (1–2) (2009) 48–56.
[39] T.D. Fornes, D.L. Hunter, D.R. Paul, Nylon-6 Nanocomposites from Alkylammonium-Modified Clay: The Role of Alkyl Tails on Exfoliation, Macromolecules 37 (5) (2004) 1793–1798.
[40] H. Zou, S. Wu, J. Shen, Polymer/silica nanocomposites: preparation, characterization, properties, and applications, Chem. Rev. 108 (2008) 3893–3957.
[41] S. Mohanty, S.K. Nayak, Effect of clay exfoliation and organic modification on morphological, dynamic mechanical, and thermal behavior of melt-compounded polyamide-6 nanocomposites, Polym. Compos. 28 (2) (2007) 153–162.
[42] D. Zheng, et al., In situ thermal reduction of graphene oxide for high electrical conductivity and low percolation threshold in polyamide 6 nanocomposites, Compos. Sci. Technol. 72 (2) (2012) 284–289.
[43] C.-W. Nan, Y. Shen, J. Ma, Physical Properties of Composites Near Percolation, Annu. Rev. Mater. Res. 40 (1) (2010) 131–151.
[44] H. Palza, C.G.O. Arias, Modifying the electrical behaviour of polypropylene/carbon nanotube composites by adding a second nanoparticle and by annealing processes, Express Polym. Lett. 6 (8) (2012) 639–646.
[45] Y. Li, et al., Poly(propylene) Nanocomposites Containing Various Carbon Nanostructures, Macromol. Chem. Phys. 212 (22) (2011) 2429–2438.
[46] S.C. Tjong, G.D. Liang, S.P. Bao, Electrical behavior of polypropylene/multi-walled carbon nanotube nanocomposites with low percolation threshold, Scr. Mater. 57 (6) (2007) 461–464.
[47] Z. Wang, et al., Synthetic methods and potential applications of transition metal dichalcogenide/graphene nanocomposites, Coord. Chem. Rev. 326 (Supplement C) (2016) 86–110.
[48] H.W. Kim, et al., Synthesis of zinc oxide semiconductors-graphene nanocomposites by microwave irradiation for application to gas sensors, Sensors Actuators B Chem. 249 (Supplement C) (2017) 590–601.
[49] S. Mallakpour, E. Khadem, Carbon nanotube–metal oxide nanocomposites: Fabrication, properties and applications, Chem. Eng. J. 302 (Supplement C) (2016) 344–367.